적응제어와 슬라이딩제어를 이용한 영구자석 동기전동기의 비선형 강인제어

백 인철, 김 경화, 윤 명중
전기 및 전자공학과
한국 과학기술원

Robust Nonlinear Speed Control of PM Synchronous Motor using Adaptive and Sliding Mode Control Techniques

In-Cheol Baik, Kyeong-Hwa Kim, and Myung-Joong Youn

Department of Electrical Engineering
Korea Advanced Institute of Science and Technology

ABSTRACT

A DSP-based nonlinear speed control of a permanent magnet synchronous motor(PMSM) which is robust to unknown parameter variations and speed measurement error is presented. The model reference adaptive system(MRAS) based adaptation mechanisms for the estimation of slowly varying parameters are derived using the Lyapunov stability theory. For the disturbances or quickly varying parameters, a quasi-linearized and decoupled model including the influence of parameter variations and speed measurement error on the nonlinear speed control of a PMSM is derived. Based on this model, a boundary layer integral sliding mode controller to improve the robustness and performance of a PMSM drive is designed and compared with the conventional controller. To show the validity of the proposed control scheme, simulations and experimental works are carried out and compared with the conventional control scheme.

I INTRODUCTION

PMSM drives are being increasingly used in a wide range of applications due to their high power density, large torque to inertia ratio, and high efficiency. This paper deals with the nonlinear speed control of a surface mounted permanent magnet synchronous motor with sinusoidal flux distribution. Since the dynamics of the currents are much faster than that of the mechanical speed, the speed is considered as a constant parameter rather than a state variable and they can be approximately linearized by the field orientation and current control [1-4]. However, this approximate linearization leads to the lack of torque due to the incomplete current control during the speed transient and reduces the control performance in some applications such as industrial robots and machine tools [5-6].

A solution to overcome this problem proposed by Le Pioufle [7] is to consider the motor speed as a state variable in electrical equations, which results in a nonlinear model. Then the nonlinear control method, so called a feedback linearization technique, is applied to obtain a linearized and decoupled model and the linear design technique is employed to complete the control design [8]. Since the nonlinear controller is very sensitive to the speed measurement error, even small measurement error results in a significant speed error and its robustness can be improved by carefully selecting the gains in the linear control loops [7]. However, besides the speed measurement error, there are parameter variations such as the stator resistance, flux, and inertia due to the temperature rise and load variations. The stator resistance and flux variations also show a steady state speed error and the inertia and flux variations degrade the transient performance. The steady state speed error may also go to zero by properly choosing the linear controller gains. However, the transient and steady state performances can still be significantly degraded due to the inertia and flux variations.

The feedback linearization deals with the technique of transforming the original system model into an equivalent model of a simpler form, and then employs the well-known and powerful linear design technique to complete the control design. However, it does not guarantee the robustness in the presence of parameter uncertainties or disturbances.

To overcome this problem, various control techniques such as adaptive control and sliding mode control can be considered. Generally, an adaptive control technique is superior to a sliding control in dealing with uncertainties of constant or slowly varying parameters. Conversely, a sliding control has some desirable features, such as its ability to deal with disturbances or quickly varying parameters [9]. Among the above mentioned parameters and disturbances, the resistance and flux are slowly varying parameters because their variations are mainly due to the temperature rises. On the contrary, the inertia can not be easily estimated using the adaptive technique because the load inertia can be abruptly and frequently changed due to the payload changes, etc., and its influence is only for a short transient period.

Therefore, in this paper, the MRAS-based adaptation mechanisms for the estimation of slowly varying parameters are derived using the Lyapunov stability theory. For the disturbances and quickly varying parameters, the feedback linearization technique is considered as a model-simplifying device for the robust control [9]. For this purpose, a quasi-linearized and decoupled model including the influence of inertia variation and speed measurement error on the nonlinear speed control of a PMSM is firstly derived and then the

robust control scheme employing a boundary layer integral sliding mode is designed to improve the control performance.

For the above mentioned control scheme, an information on the acceleration is needed and deduced from the load torque observer and state equation. Also, in order to make the current in the quadrature axis not exceed its maximum permissible value, a constraint on the motor current by means of a rectilinear speed asymptotic trajectory computation is imposed [7].

II NONLINEAR SPEED CONTROL of PMSM using INPUT-OUTPUT LINEARIZATION

A. Modeling of PMSM

The machine considered is a surface mounted PMSM and the nonlinear state equation in the synchronous dq reference frame can be represented as follows :

$$\frac{dx}{dt} = f(x) + Gu \tag{1}$$

where

$$x = \begin{pmatrix} x_1 \\ x_2 \\ x_3 \end{pmatrix} = \begin{pmatrix} i_d \\ i_q \\ \Omega \end{pmatrix} \tag{2}$$

$$u = \begin{pmatrix} u_1 \\ u_2 \end{pmatrix} = \begin{pmatrix} v_d \\ v_q \end{pmatrix} \tag{3}$$

$$G = \begin{pmatrix} \dfrac{1}{L_d} & 0 \\ 0 & \dfrac{1}{L_q} \\ 0 & 0 \end{pmatrix} \tag{4}$$

$$f(x) = \begin{pmatrix} f_1(x) \\ f_2(x) \\ f_3(x) \end{pmatrix} = \begin{pmatrix} -\dfrac{R}{L_d} x_1 + P\dfrac{L_q}{L_d} x_2 x_3 \\ -P\dfrac{L_d}{L_q} x_1 x_3 - \dfrac{R}{L_q} x_2 - P\dfrac{\Phi}{L_q} x_3 \\ \dfrac{3}{2} P\dfrac{\Phi}{J} x_2 - \dfrac{F}{J} x_3 - \dfrac{T_L}{J} \end{pmatrix} . \tag{5}$$

The parameters used in these equations are defined as follows:

v_d, v_q : stator voltages in the direct and quadrature axes

i_d, L_d : current and inductance in the direct axis

i_q, L_q : current and inductance in the quadrature axis

R : stator resistance

Ω : mechanical speed of motor

P : number of pole pairs

Φ : flux created by the rotor magnets

J : moment of inertia

F : viscous friction coefficient

T_L : load torque

f_1, f_2, f_3 : nonlinear terms in a PMSM model.

B. Nonlinear speed control of PMSM

In order to avoid any zero dynamics and to get a total input-output linearization, the direct axis current and mechanical speed are chosen as outputs. From eqn. 1 and the assumption that the load torque is considered to be an unknown constant, the relationship between the outputs and inputs of the model can be obtained as follows [7] :

$$\begin{pmatrix} \dfrac{di_d}{dt} \\ \dfrac{d^2\Omega}{dt^2} \end{pmatrix} = B + A \begin{pmatrix} v_d \\ v_q \end{pmatrix} \tag{6}$$

where

$$B = \begin{pmatrix} f_1 \\ \dfrac{3}{2}\dfrac{1}{J}\left\{ P\Phi f_2 - \dfrac{2}{3} F f_3 \right\} \end{pmatrix}, \quad A = \begin{pmatrix} \dfrac{1}{L_d} & 0 \\ 0 & \dfrac{3}{2}\dfrac{P\Phi}{L_q J} \end{pmatrix} . \tag{7}$$

The nonlinear control input which permits a linearized and decoupled behavior is deduced from this relationship as follows :

$$\begin{pmatrix} v_d \\ v_q \end{pmatrix} = A^{-1}\left(-B + \begin{pmatrix} v_1 \\ v_2 \end{pmatrix} \right) \tag{8}$$

where v_1 and v_2 are the new control inputs. By substituting eqn. 8 into 6, the linearized and decoupled model can be given as

$$\frac{di_d}{dt} = v_1 \tag{9}$$

$$\frac{d^2\Omega}{dt^2} = v_2 . \tag{10}$$

As the control laws for the new control inputs, the linear controller suggested by Le Pioufle becomes as follows :

$$v_1 = K_{11}(i_d^* - i_d) \tag{11}$$

$$v_2 = \frac{d^2\Omega^*}{dt^2} + K_{21}\frac{d}{dt}(\Omega^* - \Omega) + K_{22}(\Omega^* - \Omega) \tag{12}$$

where K_{11}, K_{21}, and K_{22} are the gains. Also, i_d^* and Ω^* are the tracking commands of the direct axis current and mechanical speed of a PMSM, respectively. As a result, the following error dynamics can be obtained as

$$\frac{de_1}{dt} + K_{11}e_1 = 0 \tag{13}$$

$$\frac{d^2e_2}{dt^2} + K_{21}\frac{de_2}{dt} + K_{22}e_2 = 0 \tag{14}$$

where $e_1 = i^* - i_d$, $e_2 = \Omega^* - \Omega$. The poles for the desired error dynamics can be chosen by properly selecting the gains using a binomial standard form, etc. [10]. The overall scheme of the conventional nonlinear speed control system is shown in Fig. 1.

C. Asymptotic load torque observer

In many motor drive systems, it is required to estimate an unknown load torque for the control system design and generally required to know all the inputs given to the system. However, in a real system, there are many cases where some of the inputs are unknown or inaccessible. For the unknown and inaccessible inputs, the observer was studied by Meditch and Hostetter and a 0-observer is selected for simplicity [11]. Thus, the inaccessible load torque (T_L) is assumed to be an unknown constant. For a PMSM, the system equation for a disturbance torque observer can be expressed as follows :

$$\frac{dz}{dt} = Dz + Ew , \quad y = \Omega = Cz \tag{15}$$

where

$$z = \begin{pmatrix} \Omega \\ T_L \end{pmatrix} = \begin{pmatrix} z_1 \\ z_2 \end{pmatrix}, \quad D = \begin{pmatrix} \dfrac{-F}{J} & \dfrac{-1}{J} \\ 0 & 0 \end{pmatrix},$$

-71-

$$E = \begin{pmatrix} \dfrac{3P\Phi}{2J} \\ 0 \end{pmatrix}, \quad C = (1,0), \quad w = i_q$$

and for this system, (D,C) is observable. The well-known asymptotic load torque observer can be designed as

$$\frac{d\hat{z}}{dt} = D\hat{z} + Ew + L(y - C\hat{z}) \tag{16}$$

where $\hat{z} = (\hat{\Omega}, \hat{T}_L)^T$ is the observed value and $L = (l_1, l_2)^T$ is the observer gain matrix.

III   PROPOSED CONTROL STRATEGY

A. MRAS-based estimation of slowly varying parameters

To estimate the slowly varying parameters such as the resistance and flux, the concept of model reference adaptive system(MRAS) is employed. The dynamic equation of a real quadrature axis current of a PMSM is considered as a reference model. In a similar way, the dynamic equation of an estimated quadrature axis current is considered as an adjustable model. The difference between the reference model and adjustable model can be reduced by an adaptation mechanism [12-13].

From eqn. 1, the reference model becomes

$$\frac{di_q}{dt} = -\frac{R}{L_q}i_q - P\frac{\Phi}{L_q}\Omega - P\frac{L_d}{L_q}i_d\Omega + \frac{v_q}{L_q}. \tag{17}$$

Similarly, the adjustable model can be expressed as

$$\frac{d\hat{i}_q}{dt} = -\frac{\hat{R}}{L_q}\hat{i}_q - P\frac{\hat{\Phi}}{L_q}\Omega - P\frac{L_d}{L_q}i_d\Omega + \frac{v_q}{L_q} \tag{18}$$

where $\hat{R}$ and $\hat{\Phi}$ are the estimated parameters and $\hat{i}_q$ is the estimated quadrature axis current.

To derive the parameter adaptation mechanisms, the Lyapunov stability theory is utilized. Let's define the error as $e = i_q - \hat{i}_q$. Then, from eqns. 17 and 18, the following equation can be obtained as

$$\frac{de}{dt} = -\frac{R}{L_q}e - \frac{(R - \hat{R})}{L_q}\hat{i}_q - P\frac{(\Phi - \hat{\Phi})}{L_q}\Omega$$

$$= -\frac{R}{L_q}e - \frac{\Delta R}{L_q}\hat{i}_q - P\frac{\Delta\Phi}{L_q}\Omega. \tag{19}$$

Now, let V be a Lyapunov function candidate defined as follows :

$$V(e, \hat{R}, \hat{\Phi}) = \frac{1}{2}\left\{ e^2 + \frac{1}{\gamma_1}\frac{(R - \hat{R})^2}{L_q} + \frac{1}{\gamma_2}\frac{(\Phi - \hat{\Phi})^2}{L_q} \right\} \tag{20}$$

where γ_1 and γ_2 are the adaptation gains which are strictly positive real.
Then, the time derivative of V becomes

$$\frac{dV}{dt} = -\frac{R}{L_q}e^2 - \frac{1}{\gamma_1}\frac{(R - \hat{R})}{L_q}\left(\gamma_1\hat{i}_qe + \frac{d\hat{R}}{dt}\right)$$

$$- \frac{1}{\gamma_2}\frac{(\Phi - \hat{\Phi})}{L_q}\left(\gamma_2\Omega e + \frac{d\hat{\Phi}}{dt}\right). \tag{21}$$

From eqn. 21, the adaptation mechanisms can be obtained by equating the second and third terms of the right hand side to zeroes as

$$\frac{d\hat{R}}{dt} = -\gamma_1\hat{i}_qe, \quad \frac{d\hat{\Phi}}{dt} = -\gamma_2\Omega e. \tag{22}$$

During the operation, the real quadrature axis current is continuously compared with the estimated quadrature axis current. The error is used in adaptation mechanisms which adjust the parameters used for the feedback linearization as shown in Fig. 2.

B. Effects of parameter estimation errors

From eqns. 21 and 22, the time derivative of the Lyapunov function candidate V can be written as

$$\frac{dV}{dt} = -\frac{R}{L_q}e^2 \leq 0. \tag{23}$$

Since the time derivative of V is negative semidefinite, it follows that e, ΔR, and $\Delta\Phi$ are bounded. In steady state, the relationship between parameter estimation errors can be given as

$$\Delta R \cdot \hat{i}_q + \Delta\Phi \cdot P\Omega = 0. \tag{24}$$

This implies that ΔR and $\Delta\Phi$ are not linearly independent and do not necessarily converge to zeroes. The steady state estimation errors of these parameters are of opposite sign.

Fig. 3 shows the typical effects of $\Delta\Phi$ and corresponding ΔR on the steady state speed error when the speed command is 1000 RPM. As shown in this figure, the effects of ΔR and $\Delta\Phi$ are canceled each other. Therefore, it can be concluded that the effects of the variations of the slowly varying parameters are effectively compensated even though there are some small estimation errors.

C. Quasi-linearized and decoupled model

For the quickly varying parameter and disturbances, the actual nonlinear control law which employs the nominal parameter values and measured mechanical speed is expressed as follows [7] :

$$\begin{pmatrix} v_d \\ v_q \end{pmatrix} = A_o^{-1}\left(-B_o + \begin{pmatrix} v_1' \\ v_2' \end{pmatrix}\right) \tag{25}$$

where v_1' and v_2' are the new control inputs, A_o and B_o are obtained from eqn. 7 using the nominal parameter values and measured speed. By substituting eqn. 25 into 6, a quasi-linearized and decoupled model including only the effect of inertia variation and speed measurement error can be obtained as follows :

$$\frac{di_d}{dt} = -P\frac{L_q}{L_d}i_q(\Omega_o - \Omega) + v_1' = f_{n1}(x) + v_1' \tag{26}$$

$$\frac{d^2\Omega}{dt^2} = -\frac{F}{J}(f_3 - f_{3o}) + \frac{3}{2}P\frac{\Phi}{J}\left(\frac{P}{L_q}(\Omega_o - \Omega)\right.$$

$$\left. + P\frac{L_d}{L_q}i_d(\Omega_o - \Omega)\right) + \frac{J_o}{J}v_2' = f_{n2}(x) + bv_2' \tag{27}$$

where the subscript " o " denotes the nominal parameter value and measured mechanical speed of motor. Unlike the linearized and decoupled model of eqns. 9 and 10, there are unwanted nonlinear terms, $f_{n1}(x)$ and $f_{n2}(x)$, and the control input gain b.

The unwanted nonlinear terms, $f_{n1}(x)$ and $f_{n2}(x)$, are not exactly known but can be estimated as $\hat{f}_{n1}(x)$

and $\hat{f}_{n2}(x)$, and the estimation errors are bounded by some known functions, $F_{n1}(x)$ and $F_{n2}(x)$, respectively. The control input gain b is also unknown but its bound can be deduced. Now, the feedback linearization technique is considered as a model-simplifying device for the robust control [9], and the control laws for the new control inputs v_1' and v_2' are derived using a boundary layer integral sliding mode control technique to overcome the drawbacks of the conventional nonlinear control scheme.

D. Control strategy for the quasi-linearized and decoupled model

Assume the bounds of parameter variations and speed measurement error are as follows :

$J = \alpha J_o$, $\alpha_{min}(=1.) \le \alpha \le \alpha_{max}(=4.)$

$\Omega = \beta \Omega_o$, $\beta_{min}(=0.95) \le \beta \le \beta_{max}(=1.05)$. (28)

Using eqn. 28, the estimates $\hat{f}_{n1}(x)$ and $\hat{f}_{n2}(x)$, and error bounds $F_{n1}(x)$ and $F_{n2}(x)$ for the quasi-linearized and decoupled model can be obtained as follows :

$$\hat{f}_{n1} = -P\frac{L_q}{2L_d}i_q(2-\beta_{min}-\beta_{max})\Omega_o \quad (29)$$

$$F_{n1} = \mid P\frac{L_q}{2L_d}i_q(\beta_{max}-\beta_{min})\Omega_o \mid \quad (30)$$

$$\hat{f}_{n2} = \frac{1}{2}\{\frac{3}{2}PFi_q\frac{\hat{\Phi}}{J_o^2}(\frac{2}{\alpha_{min}}-\frac{1}{\alpha_{min}^2}-\frac{1}{\alpha_{max}\alpha_{min}})$$

$$+\frac{F^2\Omega_o}{J_o^2}(\frac{\beta_{min}}{\alpha_{min}\alpha_{max}}-\frac{2}{\alpha_{min}}+\frac{\beta_{max}}{\alpha_{min}^2})$$

$$+\frac{F\hat{T}_L}{J_o^2}(\frac{1}{\alpha_{min}\alpha_{max}}-\frac{2}{\alpha_{min}}+\frac{1}{\alpha_{min}^2})\}$$

$$+\frac{1}{2}\{\frac{3}{2}P\frac{\hat{\Phi}}{J_o}\{\frac{1}{\alpha_{min}}P\frac{L_d}{L_q}(1-\beta_{max})\Omega_o i_d$$

$$+\frac{1}{\alpha_{min}}P\frac{(1-\beta_{max})}{L_q}\hat{\Phi}\Omega_o$$

$$+\frac{1}{\alpha_{min}}P\frac{L_d}{L_q}(1-\beta_{min})\Omega_o i_d$$

$$+\frac{1}{\alpha_{min}}P\frac{(1-\beta_{min})}{L_q}\hat{\Phi}\Omega_o\}\} \quad (31)$$

$$F_{n2} = \mid \frac{1}{2}\{\frac{3}{2}PFi_q\frac{\hat{\Phi}}{J_o^2}(\frac{1}{\alpha_{min}^2}-\frac{1}{\alpha_{max}\alpha_{min}})$$

$$+\frac{F^2\Omega_o}{J_o^2}(-\frac{\beta_{min}}{\alpha_{min}\alpha_{max}}+\frac{\beta_{max}}{\alpha_{min}^2})$$

$$+\frac{F\hat{T}_L}{J_o^2}(-\frac{1}{\alpha_{min}\alpha_{max}}+\frac{1}{\alpha_{min}^2})\}$$

$$+\frac{1}{2}\{\frac{3}{2}P\frac{\hat{\Phi}}{J_o}\{-\frac{1}{\alpha_{min}}P\frac{L_d}{L_q}(1-\beta_{max})\Omega_o i_d$$

$$-\frac{1}{\alpha_{min}}P\frac{(1-\beta_{max})}{L_q}\hat{\Phi}\Omega_o$$

$$+\frac{1}{\alpha_{min}}P\frac{L_d}{L_q}(1-\beta_{min})\Omega_o i_d$$

$$+\frac{1}{\alpha_{min}}P\frac{(1-\beta_{min})}{L_q}\hat{\Phi}\Omega_o\}\}\mid. \quad (32)$$

The bound on the control input gain is

$$b_{min}\left(=\frac{1}{\alpha_{max}}=0.25\right)\le b \le b_{max}\left(=\frac{1}{\alpha_{min}}=1.0\right). \quad (33)$$

Using eqns. 29 through 33, the design problem of the sliding mode controller for the quasi-linearized and decoupled model of eqns. 26 and 27 is well introduced in a previous work [9]. The boundary layer integral sliding mode controller is considered to avoid the chattering phenomenon and the reaching phase problem [9, 14-15]. The sliding surface s_1 is chosen as

$$s_1 = \left(\frac{d}{dt}+\lambda_1\right)\int^t e_1 dt = e_1 + \lambda_1\int_0^t e_1 dt - e_1(0). \quad (34)$$

The control law for v_1' is designed to guarantee $s_1\dot{s}_1 < -\eta_1|s_1|$ as

$$v_1' = \hat{v}_1 - k_1 sat\left(\frac{s_1}{\Phi_1}\right) \quad (35)$$

where $\hat{v}_1 = -\hat{f}_{n1}-\lambda_1 e_1$, $k_1 = F_{n1}+\eta_1$, and $sat(\cdot)$ is the saturation function. Also, λ_1 and η_1 are the strictly positive constants. From eqn. 34, it can be noted that $s_1 = 0$ from time $t = 0$ and there is no reaching phase problem.

From the bound on the control input gain b of eqn. 33, the geometric mean b_m can be defined as

$$b_m = (b_{max}b_{min})^{1/2} = \left(\frac{1}{\alpha_{max}\alpha_{min}}\right)^{1/2}. \quad (36)$$

The bound on b can then be written as

$$\Psi^{-1} \le \frac{b_m}{b} \le \Psi \quad (37)$$

where

$$\Psi = \left(\frac{b_{max}}{b_{min}}\right)^{1/2} = \left(\frac{\alpha_{max}}{\alpha_{min}}\right)^{1/2}.$$

The sliding surface s_2 is chosen as

$$s_2 = \left(\frac{d}{dt}+\lambda_2\right)^2\int^t e_2 dt = \frac{de_2}{dt}+2\lambda_2 e_2$$

$$+\lambda_2^2\int_0^t e_2 dt - \frac{de_2}{dt}\mid_{t=0}-2\lambda_2 e_2(0). \quad (38)$$

The control law for v_2' is also designed to guarantee $s_2\dot{s}_2 < -\eta_2|s_2|$ as

$$v_2' = b_m^{-1}\left(\hat{v}_2 - k_2 sat\left(\frac{s_2}{\Phi_2}\right)\right) \quad (39)$$

where

$\hat{v}_2 = -\hat{f}_{n2} - 2\lambda_2 de_2 / dt - \lambda_2^2 e_2$,

$k_2 = \Psi(F_{n2}+\eta_2)+(\Psi-1)|\hat{v}_2|$, λ_2 and η_2 are strictly positive constants. From eqn. 38, it can also be noted that $s_2 = 0$ from time $t = 0$ and there is no reaching phase problem.

The bounds of uncertainties needed for the robust nonlinear control are obtained by deriving a quasi-linearized and decoupled model, and the robustness can be achieved by applying these bounds to generate the control inputs which compensate the parameter uncertainties and speed measurement error. The overall scheme of the proposed robust nonlinear speed control system is shown in Fig. 4.

IV Simulations and experimental results

A. System configuration

The simulations and experimental works are carried out for the PMSM with the specifications listed as in Table 1.

The configuration of the DSP-based experimental system is shown in Fig. 5. The main processor of the experimental system is a floating point Digital Signal Processor TMS320C30 with a clock frequency of 32MHz [16-17]. The PMSM is driven by a three phase voltage source PWM inverter using an intelligent power module with a switching frequency of 7.8 kHz. The brushless resolver and resolver to digital converter are used to detect the absolute rotor position and speed of the PMSM. The resolution of detected position is selected as 12 bits. The phase currents are detected by the Hall-effect devices and the measured analogue signals are converted to digital values using the Analog to Digital converter with a 12 bit resolution. The PWM gate firing signals for the desired phase voltage commands are generated by using the space vector modulation technique [18]. The sampling period of the control system is set as 128 μ sec.

To examine the performance of the proposed control scheme, the dynamic behavior of the control system is tested under the inertia or flux variations in the acceleration region with the acceleration time of 50 msec.

B. Simulation results

To show the validity of the proposed control scheme, the computer simulations are carried out for the systems shown in Figs. 1 and 4 under various conditions. Fig. 1 shows the overall block diagram of the conventional nonlinear speed controller and Fig. 4 shows the proposed robust nonlinear speed controller. The design parameters used for the conventional nonlinear control scheme are selected as $K_{11} = 2100$, $K_{21} = 700$, and $K_{22} = 490000$ to obtain nearly the same performances as those of the proposed control scheme when there are no parameter variations or disturbances. For the proposed robust nonlinear control scheme, the design parameters are selected as $\gamma_1 = \gamma_2 = 0.5$, $\lambda_1 = 2100$, $\lambda_2 = 700$, $\eta_1 = 1$, $\eta_2 = 10$, $\phi_1 = 0.005$, and $\phi_2 = 10000$. It can be noted from eqn. 38 that the sliding surface is a weighted sum of terms related to a tracking error and the large boundary layer thickness does not mean a large tracking error [9]. The observer gains are selected as $l_1 = 796.67$ and $l_2 = -21.024$ to locate the double observer poles at - 400 when there are no parameter variations. Figs. 6(a) and (b) show the speed response and quadrature axis current under no inertia variation($J = J_o$) for both control schemes. Figs. 7(a) and (b) show the same phenomena under the inertia variation of 4 times the nominal value($J = 4J_o$). As shown in these figures, the conventional nonlinear control scheme shows a significant degradation in the transient response. Under the inertia variation of 4 times the nominal value, it shows the enhanced overshoot of 5.5% and prolonged settling time of 75msec. However, the proposed robust nonlinear control scheme shows a good performance without such a degradation. Fig. 8 shows the case of inertia variation of 4 times the nominal value and +30% flux variation. As shown in this figure, the conventional

scheme shows the enhanced overshoot of 16% and steady state speed error. It can be noted from this figure that the additional degradations in the transient and steady state responses are occurred due to flux uncertainties. However, the proposed robust nonlinear control scheme shows a good performance without such degradations.

C. Experimental results

The experimental works are carried out for the conventional and proposed control schemes. The same design parameters given in the previous section are used in both control schemes. The dynamic responses under the various conditions are shown in Figs. 9-14. As shown in Fig. 9, both control schemes provide good dynamic responses corresponding to the design specifications when there is no inertia variation($J = J_o$). However, when the inertial load is increased($J = 4J_o$), the overshoot and settling time in the conventional nonlinear control scheme are increased up to 6% and 70msec as shown in Fig. 10(a). On the other hand, the proposed robust nonlinear control scheme provides nearly the same responses for both cases as shown in Figs. 9(b) and 10(b). For the case of inertia variation of 4 times the nominal value and +30% flux variation, the conventional control scheme shows the increased overshoot of 16% and steady state speed error as shown in Fig. 11(a). However, the proposed control scheme provides a good response as shown in Fig. 11(b). It can be observed from the experimental results in Figs. 9(b), 10(b), and 11(b) that there are no control chatterings in the quadrature axis currents by employing the boundary layers [9]. Even though some differences exist between simulations and experimental results mainly due to the unknown friction coefficient, etc., it can be considered that the above simulations and experimental results well verify the validity of the proposed robust nonlinear control scheme.

Fig. 12 shows the estimated flux for the proposed control scheme when there is +30% flux variation. As shown in this figure, it can be said that the parameter estimation scheme shows a reasonable performance. Fig. 13 shows the values of sliding surfaces s_1 and s_2 during speed transient for the proposed control scheme when there are inertia variation of 4 times the nominal value and +30% flux variation. It can be noted that the values of sliding surfaces are bounded within the boundary layers and these values are zeroes at the beginning of control actions. Therefore, it can be said that the sliding conditions are satisfied from the beginning of control actions without reaching phase problems. The values of sliding surfaces s_1 and s_2 at steady state are shown in Fig. 14 when there are inertia variation of 4 times the nominal value and +30% flux variation. It can be noted that the value of sliding surface s_2 is decreased to a small value in the boundary layer at steady state.

V Conclusion

This paper proposes a robust nonlinear speed control scheme for a PMSM which guarantees the robustness in the presence of parameter variations and speed measurement error. The MRAS-based adaptation mechanisms for the estimation of slowly varying parameters are derived using the Lyapunov stability theory. For the quickly varying parameters and

disturbances, the influence of parameter variations and speed measurement error on the nonlinear speed control of a PMSM is investigated and a quasi-linearized and decoupled model is derived. Based on this model, the design methods for the proposed control scheme have been given using the boundary layer integral sliding mode control technique. The bounds of uncertainties needed for the sliding mode control are deduced and the robustness is achieved by using these bounds to generate the control inputs which compensate the parameter uncertainties and disturbances. By introducing the boundary layer integral sliding mode technique, the chattering phenomenon can be reduced and the reaching phase problem can be avoided.

To show the validity of the proposed control scheme, the comparative simulations and experimental works have been carried out under various conditions. Compared with the conventional nonlinear control scheme, the proposed robust nonlinear control scheme provides good transient and steady state performances under the inertia and flux variations. For the proposed control scheme, the MRAS-based adaptation mechanisms for the estimation of slowly varying parameters show reasonable performances. Also, the chattering phenomenon can be reduced and the reaching phase problem can be avoided by introducing the boundary layer integral sliding mode technique. It can be said from these results that the proposed control scheme has the robustness against the unknown disturbances. Therefore, it can be expected that the proposed control scheme can be applied to the high performance applications such as the machine tools and industrial robots.

REFERENCES

1   CHAMPENOIS, G., MOLLARD, P., and ROGNON, J. P.: 'Synchronous servo drive: a special application'. *IEEE-IAS Conf. Rec.*, 1986, pp. 182-189

2   FADEL, M., and DE FORNEL, B.: 'Control laws of a synchronous machine fed by a PWM voltage source inverter'. *EPE*, Aachen, RFA, Oct. 1989

3   LEONHARD, W.: 'Control of electrical drives' (Springer Verlag,1985)

4   REKIOUA, T., MEIBODY TABAR, F., CARON, J. P., and LE DOEUFF, R.: 'Study and comparison of two different methods of current control of a permanent magnet synchronous motor'. *Conf. Rec. IMACS-TCI*, Nancy, France, 1990, 1, pp. 157-163

5   LE PIOUFLE, B., and LOUIS, J. P., 'Influence of the dynamics of the mechanical speed of a synchronous servomotor on its torque regulation, proposal of a robust solution', *EPE*, Florence, 1991, 3, pp. 412-417

6   CARROLL JR. J. J., and DAWSON, D. M.: 'Integrator backstepping techniques for the tracking control of permanent magnet brush DC motors', *IEEE Trans. IA*, 1995, IA-31, (2), pp. 248-255

7   LE PIOUFLE, B.: 'Comparison of speed nonlinear control strategies for the synchronous servomotor', *Electric Machines and Power Systems*, 1993, 21, pp. 151-169

8   ISIDORI, A.: 'Nonlinear control systems: an introduction' (Springer-Verlag, 1985)

9   SLOTINE, J. J., and LI, W.: 'Applied nonlinear control' (Prentice-Hall, 1991)

10   NAGRATH, I. J., and GOPAL, M.: 'Control systems engineering' (John Wiley & Sons, 1982)

11   MEDITCH, J., and HOSTETTER, G.: 'Observers for systems with unknown and inaccessible inputs', *Int. J. Control*, 1974, 19, (3), pp. 473-480

12   NARENDRA, K. S., and ANNASWAMY, A. M.: 'Stable adaptive systems' (Prentice-Hall, 1989)

13   ASTROM, K. J., and WITTENMARK, B.: 'Adaptive control' (Addison Wesley, 1995)

14   CHERN, T. L., and WU, Y. C.: 'Design of brushless DC position servo systems using integral variable structure approach', *IEE proc.-B*, 1993, 140, (1), pp. 27-34

15   LEE, J. H., KO, J. S., CHUNG, S. K., LEE, D. S., LEE, J. J., and YOUN, M. J.: 'Continuous variable structure controller for BLDDM with prescribed tracking performance', *IEEE Trans. IE*, 1994, IE-41, (5), pp. 483-491

16   TMS320C3X User's Guide, Texas Instruments Inc., 1990

17   TMS320C30 Assembly Language Tools User's Guide, Texas Instruments Inc., 1990

18   KENJO, T.: 'Power Electronics for the Microprocessor Age' (Oxford University Press, 1990)

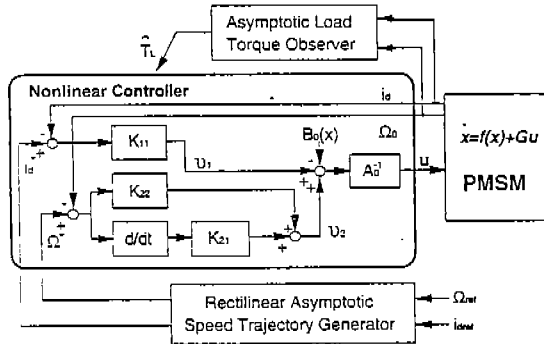| Rated Power	400 W	Rated Speed	3000 RPM
Rated Torque	1.274 Nm	Rated Voltage	190 V
Number of Pole Pairs	2	Flux Linkage	0.167 Wb
Stator Resistance	3 Ohm	Stator Inductance	7 mH
Moment of Inertia	$1.314 \cdot 10^{-4}$ Nmsec^2		

Table 1. Specifications of PMSM

Fig. 1. Block diagram of the conventional nonlinear control scheme
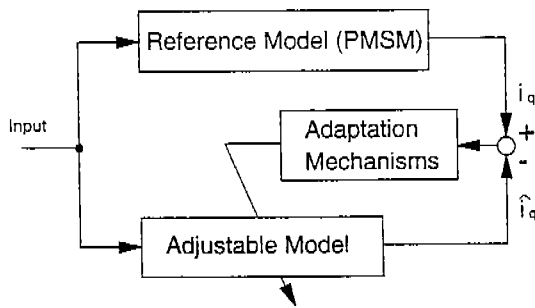

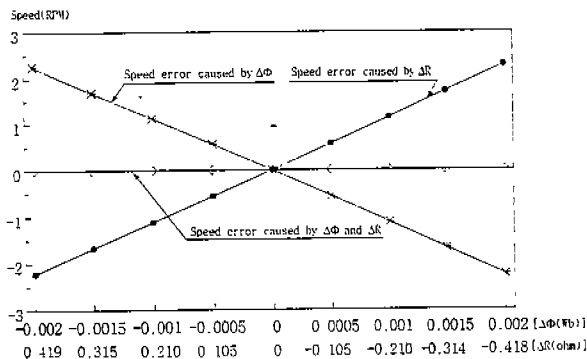Fig. 2. Block diagram of MRAS-based parameter estimation scheme

Fig. 3. Steady state speed error caused by estimation errors of flux and corresponding resistance
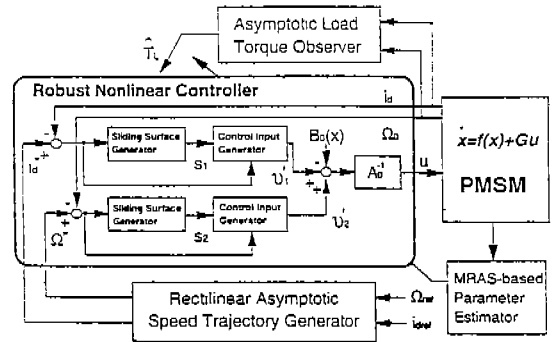
Fig. 4. Block diagram of the proposed robust nonlinear control scheme
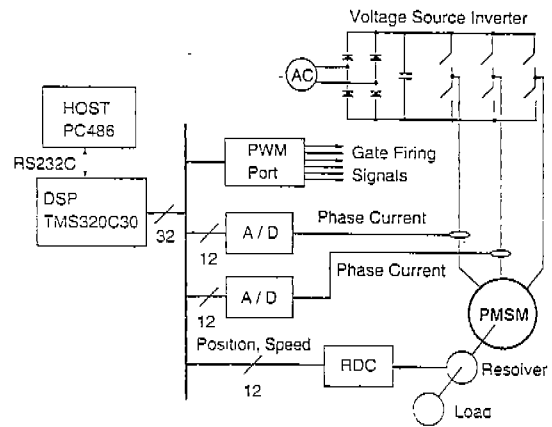
Fig. 5. Configuration of DSP-based experimental system
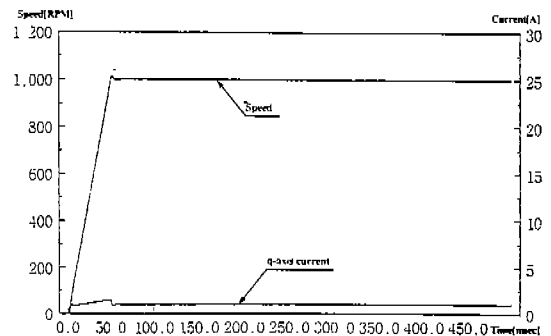
(a) Conventional control scheme
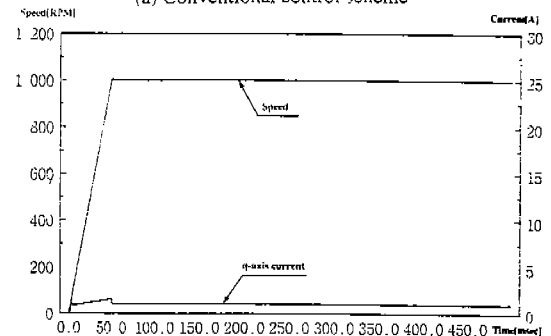
(b) Proposed control scheme

Fig. 6. Speed response and q-axis current under no inertia variation
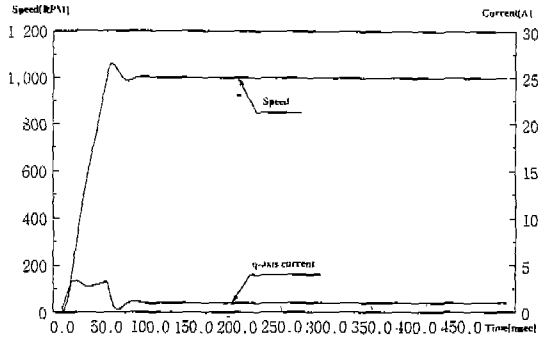
(a) Conventional control scheme
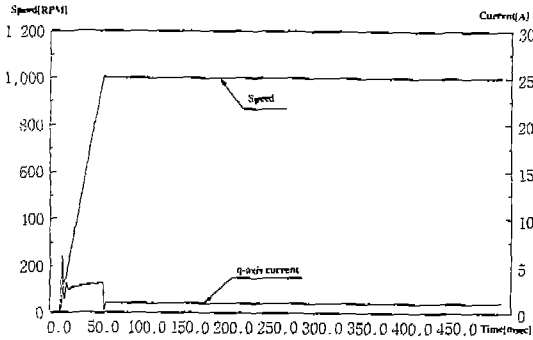
(b) Proposed control scheme

Fig. 7. Speed response and q-axis current under inertia variation($J = 4J_o$)
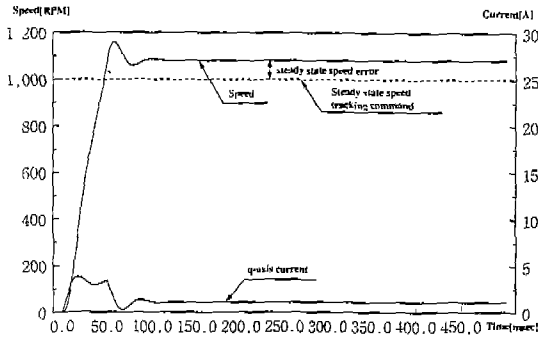
(a) Conventional control scheme
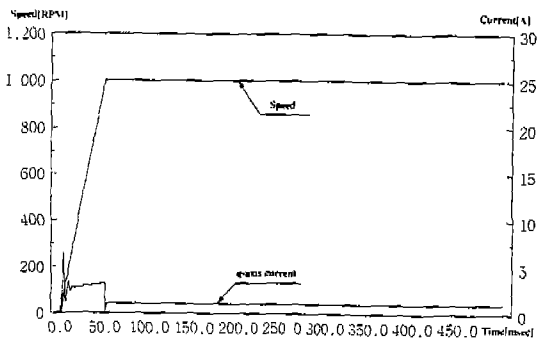
(b) Proposed control scheme

Fig. 8. Speed response and q-axis current under inertia variation($J = 4J_o$) and +30% flux variation
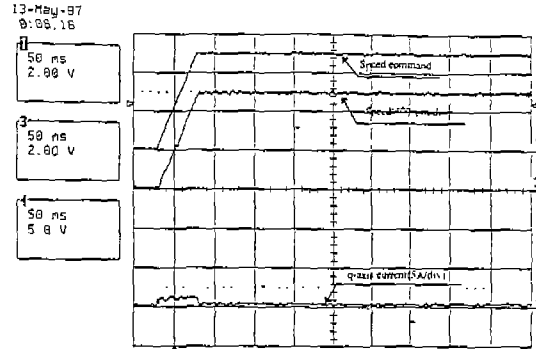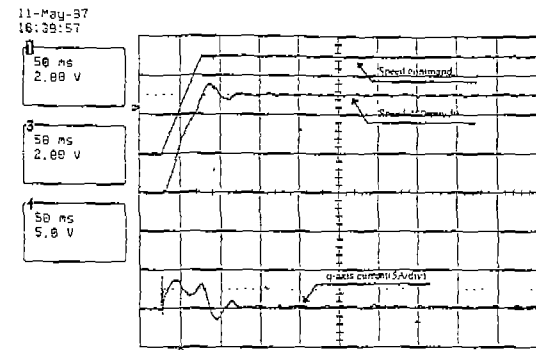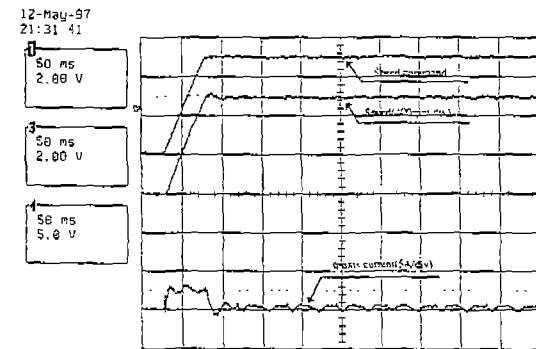

(a) Conventional control scheme
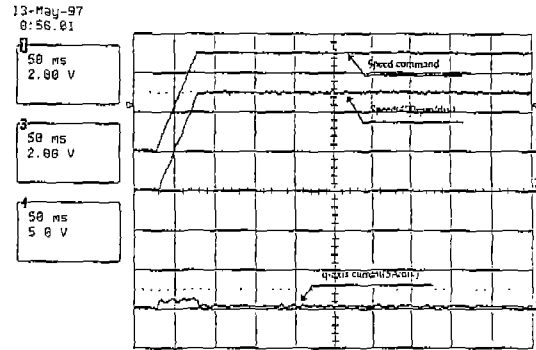
(b) Proposed control scheme

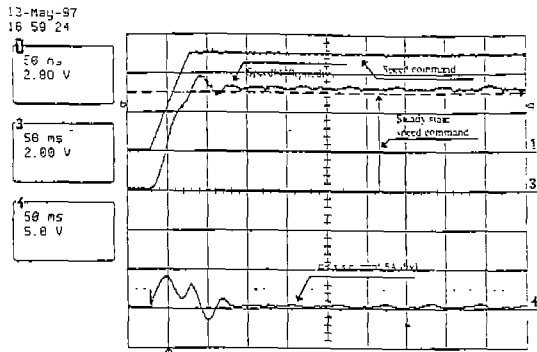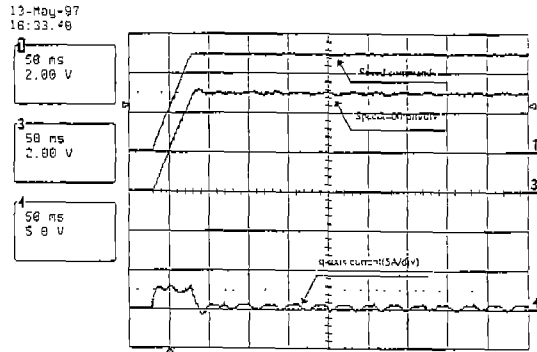Fig. 9. Speed response and q-axis current under no inertia variation [experiments]

(a) Conventional control scheme

(b) Proposed control scheme

Fig. 10. Speed response and q-axis current under inertia variation($J = 4J_o$) [experiments]

(a) Conventional control scheme

(b) Proposed control scheme

Fig. 11. Speed response and q-axis current under inertia variation($J = 4J_o$) and +30% flux variation [experiments]
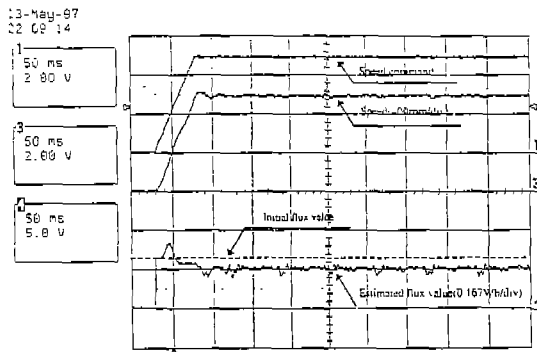

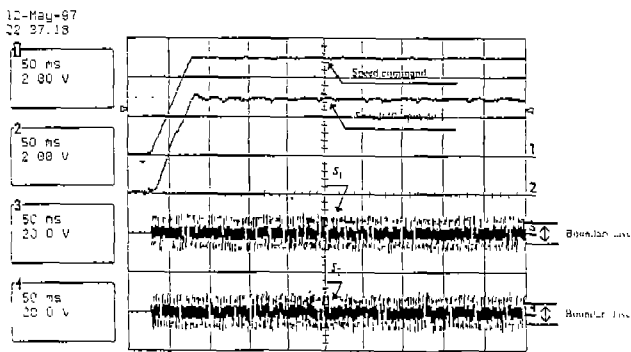Fig. 12. Value of estimated flux under +30% flux variation [experiment]

Fig. 13. Values of sliding surfaces s_1 and s_2 during speed transient under inertia variation($J = 4J_o$) and +30% flux variation [experiment]
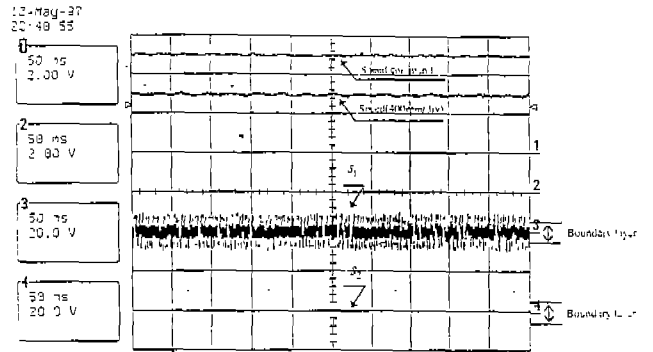

Fig. 14. Values of sliding surfaces s_1 and s_2 under inertia variation($J = 4J_o$) and +30% flux variation at steady state [experiment]